Published in final edited form as:
J Med Chem. 2011 December 22; 54(24): 8451–8460. doi:10.1021/jm200982p.

C-terminal tetrapeptides inhibit Aβ42-induced neurotoxicity primarily through specific interaction at the N-terminus of Aβ42

Huiyuan Li[≠], **Zhenming Du**[&], **Dahabada H. J. Lopes**[≠], **Erica A. Fradinger**[≠,§], **Chunyu Wang**[&], and **Gal Bitan**[≠,¶,ʃ,*]

[≠]Department of Neurology, David Geffen School of Medicine, University of California, Los Angeles, 635 Charles E. Young Drive S., Los Angeles, CA, 90095

[¶]Brain Research Institute, University of California, Los Angeles, 635 Charles E. Young Drive S., Los Angeles, CA, 90095

[ʃ]Molecular Biology Institute, University of California, Los Angeles, 635 Charles E. Young Drive S., Los Angeles, CA, 90095

[&]Department of Biology, Rensselaer Polytechnic Institute, 110 8th Street, Troy, NY 12180

Abstract

Inhibition of amyloid β-protein (Aβ)-induced toxicity is a promising therapeutic strategy for Alzheimer's disease (AD). Previously, we reported that the C-terminal tetrapeptide Aβ(39–42) is a potent inhibitor of neurotoxicity caused by Aβ42, the form of Aβ most closely associated with AD. Here, initial structure-activity relationship studies identified key structural requirements, including chirality, side-chain structure, and a free N-terminus, which control Aβ(39–42) inhibitory activity. To elucidate the binding site(s) of Aβ(39–42) on Aβ42, we used intrinsic tyrosine (Y) fluorescence and solution-state NMR. The data suggest that Aβ(39–42) binds at several sites, of which the predominant one is located in the N-terminus of Aβ42, in agreement with recent modeling predictions. Thus, despite the small size of Aβ(39–42) and the hydrophobic, aliphatic nature of all four side-chains, the interaction of Aβ(39–42) with Aβ42 is controlled by specific intermolecular contacts requiring a combination of hydrophobic and electrostatic interactions and a particular stereochemistry.

Keywords

Alzheimer's disease; amyloid β-protein; C-terminal fragment; tetrapeptide; structure-activity relationship; NMR; toxicity; intrinsic fluorescence

[*]To whom correspondence should be addressed: Department of Neurology, David Geffen School of Medicine, University of California at Los Angeles, Neuroscience Research Building 1, Room 451, 635 Charles E. Young Dr. South, Los Angeles, CA 90095-7334. gbitan@mednet.ucla.edu. Telephone: (310) 206-2082. Fax: (310) 20 700.
[§]Current address: Department of Biology, Whittier College, 13406 E Philadelphia St., Whittier, CA, 90608

Supporting Information Available

Fig. S1 presenting dose-response inhibition of Aβ42-induced toxicity by Aβ(39–42) analogues, Fig. S2 presenting the change in intrinsic fluorescence of each Y-substituted Aβ42 analogue upon addition of Aβ(39–42) and derivatives, Fig. S3 presenting the fluorescence change of [Y1]Aβ42 upon addition of each Aβ(39–42) derivative, and Figs. S4 and S5 presenting the chemical shift of Aβ42 in solution-state, 2D-NMR in the absence and presence of Ac-VVIA or vvia are available free of charge via the Internet at http://pubs.acs.org.

Introduction

Neurotoxic oligomers of amyloid β-protein (Aβ) are believed to be the main cause of Alzheimer's disease (AD).[1–4] Two predominant forms of Aβ, comprising 40 (Aβ40) or 42 (Aβ42) amino acid residues, are produced *in vivo*. Aβ42 has been shown to be more neurotoxic than Aβ40,[5] and to follow a different pathway of oligomerization.[6,7] Aβ42 forms higher-order metastable oligomers than Aβ40 and this tendency correlates with structural stabilization of the C-terminus of Aβ42 mediated by the presence of I41 and A42.[6,8–10]

Inhibition of Aβ aggregation by short peptides derived from the sequence of Aβ itself has been used by a number of groups, primarily along the idea of "β-sheet breaker" peptides that interfere with formation of the characteristic β-sheet-rich amyloid fibrils. The most utilized sequence for this line of investigation has been the central hydrophobic cluster of Aβ (CHC, residues 17–21),[11–16] which is a key region in Aβ fibrillogenesis.[17] Utilizing a similar strategy, recently, rationally designed aminopyrazole-based β-sheet breakers were found to inhibit Aβ assembly and toxicity, with the most effective inhibitor being a conjugate of aminopyrazole and the CHC-derived sequence LPFFD.[18] Using a different Aβ region for inhibitor design, modified Aβ42 C-terminal fragments, GVVIA-NH_2 and RVVIA-NH_2, were designed as β-sheet breakers and partially protected SH-SY5Y neuroblastoma cells from Aβ42 neurotoxicity in cell viability,[19] but not electrophysiological assays.[20] In a different study, hexapeptides derived from Aβ(32–37) with varying extent of N-methylation were found to retard β-sheet and fibril formation and reduce Aβ neurotoxicity.[21]

As evidence emerged ascribing pathogenic primacy to Aβ oligomers rather than fibrils,[22] inhibitor-design efforts have shifted towards inhibition of Aβ oligomerization. Guided by the principle of self-recognition and considering the critical role of the C-terminal region of Aβ42 in self-assembly,[6,8] we prepared C-terminal fragments (CTFs) of the general formula Aβ(x–42), x = 28–39, and evaluated their capability to disrupt the assembly and neurotoxicity of Aβ42.[23] Of the 12 CTFs tested, the shortest one, Aβ(39–42), had surprisingly high activity. Aβ(39–42) was found to inhibit Aβ42-induced neurotoxicity in differentiated rat pheochromocytoma (PC-12) cells with half-maximal (IC_{50}) values of 16 ± 5 and 47 ± 14 μM using the (3-(4,5-dimethylthiazol-2-yl)-2,5-diphenyltetrazolium bromide (MTT) reduction and lactate dehydrogenase (LDH) release assays, respectively.[23] In addition, Aβ(39–42) significantly rescued mouse primary hippocampal neurons from Aβ42-induced inhibition of miniature excitatory postsynaptic current frequency.[23] The data suggested that Aβ(39–42) inhibited Aβ42-induced toxicity both in the early stage of synaptic activity and in later stages of metabolism deficits and cell death.

In follow-up dynamic light scattering studies, we found that Aβ(39–42) stabilized oligomers with a hydrodynamic radius of 6±3 nm and 30±10 nm, which we interpreted as resulting from formation of heterooligomers comprising both Aβ42 and Aβ(39–42).[23,24] Computer modeling of Aβ(39–42) co-assembled with Aβ42 supported the formation of heterooligomers and suggested that Aβ(39–42) binds near the N-terminal region, Aβ(2–4), and sequesters this region from the aqueous milieu.[23,25]

The amphipathic nature and small size of Aβ(39–42) make its pharmacokinetic characteristics close to recommended values of drug-like criteria, including Lipinski's Rule of 5[26] and topological polar surface area (tPSA)[27] (Table 1), supporting its development as a drug lead. Towards this end, here we performed structure-activity relationship (SAR) studies to delineate structural features important for inhibitory activity and characterized the binding of Aβ(39–42) to Aβ42 using intrinsic fluorescence and two-dimensional (2D) solution-state NMR. The data suggest that Aβ(39–42) protects cells against Aβ42-induced toxicity predominantly via specific interaction at the N-terminus of Aβ42.

Results

Structure–activity relationship study of Aβ(39–42)

To guide future rational development of Aβ(39–42) as a drug lead, we asked what structural characteristics were important for the inhibitory activity and what specific interactions controlled the binding of Aβ(39–42) to Aβ42. In search of the answers for these questions, we synthesized a series of Aβ(39–42) derivatives, including A substitution of the first three residues (**A**VI**A**, V**A**IA, VV**AA**), an inverso-peptide (vvia, lower-case letters represent *D*-configuration), the N-terminally and C-terminally protected analogues Ac-VVIA, VVIA-NH_2, a retro-peptide (AIVV), and N-terminally and C-terminally protected versions of the retro-peptide (Ac-AIVV, AIVV-NH_2) (Table 2).

We began evaluating the new derivatives by testing if these peptides themselves were toxic to differentiated PC-12 cells using the MTT assay. The results showed that all the derivatives were not toxic (Fig. 1, white bars). Notably, Aβ(39–42) and the analogues, **A**VIA, V**A**IA, VVIA-NH_2, AIVV, and AIVV-NH_2, caused a significant increase of 10–35% in cell viability relative to control cells. Next, we screened the Aβ(39–42) derivatives for inhibition of Aβ42-induced neurotoxicity in single-dose experiments. Differentiated PC-12 cells were incubated with Aβ42 for 24 h in the absence or presence of 10-fold excess of each derivative, and cell viability was assessed using the MTT assay. Among the nine derivatives tested, the same five analogues that increased cell viability on their own showed statistically significant attenuation of Aβ42-induced toxicity (Fig. 1, black bars), similar to the parent peptide. The A-substituted sequences, **A**VIA and V**A**IA, showed similar inhibitory activity to that of Aβ(39–42), whereas VV**A**A lost inhibitory activity suggesting that the side-chains of V39 (full-length Aβ numbering) and V40 were relatively insensitive to structural changes, but the side-chain of I41 was important for inhibition. However, the observation that inhibitory activity was maintained in the retro sequence, AIVV, suggested that a bulky hydrophobic side-chain in position 41, such as I or V, might be sufficient for the inhibitory activity. The loss of activity in the inverso-peptide (vvia) indicated that the chirality of Aβ(39–42) was required for inhibition of toxicity. The analogues in which the N-terminus was acetylated, Ac-VVIA and Ac-AIVV, showed no inhibitory activity, whereas the analogues with amidated C-terminus, VVIA-NH_2 and AIVV-NH_2, were as active as Aβ(39–42) indicating that a free N-terminal amino group was essential for the activity, whereas the C-terminus could be modified to provide protection from carboxyexopeptidases.

Further characterization showed that all the active derivatives inhibited Aβ42-induced toxicity dose-dependently (Table 2 and Supplementary Fig. S1). The differences among the IC_{50} values of the Aβ(39–42) derivatives in the MTT assay were relatively small and not statistically significant, except for the IC_{50} of AVIA, 53 ± 10 μM, which was significantly higher ($p = 0.0081$, Student's t-test) than that of Aβ(39–42), 21 ± 6 μM. The differences among the IC_{50} values found in the LDH assay for all the Aβ(39–42) derivatives were statistically insignificant.

Aβ(39–42) specifically inhibits Aβ42-induced toxicity

Because Aβ(39–42) and some of its analogues caused increased cell viability relative to cells treated with cell culture medium alone, we asked whether the observed inhibition of Aβ42-induced toxicity was mediated, at least partially, by a mechanism that did not involve interaction with Aβ42. To address this question, we compared the effect of Aβ(39–42) on neurotoxicity induced by Aβ42 and several other toxins. For initial examination we used staurosporine, a non-selective protein-kinase inhibitor that induces apoptosis in multiple cell types.[28] Differentiated PC-12 cells treated with 0.2 μM staurosporine or 10 μM Aβ42 showed similar decrease in cell viability in both the MTT (Fig. 2A) and the LDH (Fig. 2B)

assays. As expected, Aβ(39–42) showed dose-dependent inhibition of Aβ42-induced toxicity. In contrast, Aβ(39–42) had no effect on staurosporine-induced cell death.

One mechanism by which Aβ42 is thought to cause toxicity is disruption of the cell membrane leading to leakage of ions and/or other metabolites, either due to formation of non-specific channels[29] or via perturbation of the phospholipid bilayer conductance without channel formation.[30] To examine whether Aβ(39–42) protected the cells against membrane perturbation, we examined next its ability to protect against alamethicin, a fungal peptide antibiotic, which potently induces voltage-dependent ion channel formation in phospholipid membranes.[31] In addition, we used another amyloidogenic protein, α-synuclein, for which similar mechanisms of toxicity to Aβ42 have been proposed.[32] Differentiated PC-12 cells treated with 15 μM α-synuclein, 4 μM alamethicin, or 10 μM Aβ42 showed similar decrease in cell viability in MTT assay (Fig. 2C). Addition of increasing concentrations of Aβ(39–42) resulted in dose-dependent inhibition of the toxicity induced by Aβ42, as observed in previous experiments (Figs. 2A and S1). In contrast, only weak protection from α-synuclein- or alamethicin-induced toxicity was observed, suggesting that non-specific protection was a minor component of the inhibitory effect of Aβ(39–42), whereas the major mechanism was mediated through direct and specific interaction with Aβ42.

Binding site(s) of Aβ(39–42) on Aβ42

Originally, the hypothesis that led us to examine Aβ42 CTFs as inhibitors of Aβ42 assembly and toxicity was based on the principle of self-recognition and we predicted that the CTFs would bind to the C-terminus of Aβ42.[23,33] However, our previous investigation of the mode of interaction between the CTFs and Aβ42 suggested that different CTFs might inhibit Aβ42-induced toxicity by distinct mechanisms[23,24] and might bind Aβ42 at sites other than the C-terminus.[25] Therefore, here we used two complementary methods to elucidate the binding site(s) of Aβ(39–42), the shortest CTF in original series, on Aβ42.

Characterization of the interaction between Aβ(39–42) and Aβ42 by intrinsic Y fluorescence—Elucidation of binding sites for inhibitors of aberrant protein self-assembly is a difficult task because the self-assembly typically occurs among disordered monomers and produces metastable oligomers, in which the degree of order still is low. To explore potential binding site(s) of Aβ(39–42) on Aβ42 we took advantage of the intrinsic fluorescence of Y residues, which enables rapid signal detection at low concentrations under which minimal or no aggregation occurs during the time of the experiment (~30 min), thus measuring binding to monomers and low-order oligomers.

In addition to wild-type (WT) Aβ42, in which a single Y residue is at position 10, we used analogues in which Y substituted the original residues at positions 1, 20, 30, or 42, and the native Y10 was substituted by the fluorometrically silent F. The sequences of WT Aβ42 and its Y-substituted analogues are shown in Fig. 3A. These analogues were used previously to study Aβ42 folding and assembly.[34,35] Morphological studies by electron microscopy (EM) showed that all the Y-substituted Aβ42 analogues formed fibrils and the fibril morphologies observed were similar to those formed by WT Aβ42.[34] Secondary structure dynamics examination by circular dichroism spectroscopy showed that qualitatively all the Y-substituted analogues were predominately disordered initially, and then displayed characteristic statistical coil to a-helix to β-sheet transitions during oligomerization and fibril formation.[34]

Exposure to the aqueous milieu is known to decrease Y fluorescence intensity without altering the wavelength of maximum emission (λ_{max}). In addition, the fluorescence of the phenol group in the Y side-chain can be quenched by exposure to hydrated carbonyl groups or through hydrogen-bond formation with peptide carbonyls or with carboxylate groups in

aspartate or glutamate side-chains.[34,36] In our experimental system, an increase in Y fluorescence upon addition of Aβ(39–42) would suggest a decrease in solvent exposure, possibly indicating binding of the tetrapeptide to, or in the vicinity of, the Y residue. Alternatively, an increase in fluorescence could be interpreted as arising from increase in intra- or intermolecular interactions within or between Aβ42 monomers, respectively. However, we reasoned that changes in fluorescence resulting from global folding and/or assembly of Aβ42 likely would affect Y residues in multiple positions, whereas specific, local binding of Aβ(39–42) would lead to increased Y fluorescence only in a specific position.

To minimize Aβ aggregation during the assay, all the samples were pre-treated with 1,1,1,3,3,3-hexafluoroisopropanol (HFIP),[37,38] and measurement of fluorescence was initiated immediately following rehydration. In addition, aliquots were monitored by EM. During the time of fluorescence measurements (~30 min), all the peptides formed quasi-globular structures with diameters ranging from ~7–15 nm and no fibrils were observed. A representative electron micrograph of Aβ42 prepared under these conditions is shown in Fig. 3B. The fluorescence intensity of Aβ42 and its Y-substituted analogues is shown in Fig. 3C. Consistent with a previous report,[34] the observed trend suggested that the degree of exposure to the aqueous solvent decreased gradually from the N- to the C-terminus.

The fluorescence intensity of Aβ42 analogues (5 μM) mixed with Aβ(39–42) (50 μM) is shown in the second bar of each group in Fig. 3D. To facilitate the comparison among the five Aβ42 analogues, the fluorescence intensity in the presence of Aβ(39–42) in each case was normalized to the fluorescence of the analogue in the absence of Aβ(39–42) (first bar of each group in Fig. 3D). We found that upon addition of Aβ(39–42), the fluorescence of [Y1]Aβ42 increased by 117 ± 3%. In contrast, the fluorescence of WT Aβ42, [Y20]Aβ42, [Y30]Aβ42, and [Y42]Aβ42 did not change significantly upon addition of Aβ(39–42). These results suggested that Aβ(39–42) bound mainly at the N-terminus of Aβ42.

Because the N-terminus of Aβ contains several charged residues, we hypothesized that the charged amino- and carboxyl groups in Aβ(39–42) might be important for its binding to the N-terminus of Aβ42. To test this hypothesis, we examined the effect of Aβ(39–42) analogues in which the N- or C-termini were blocked by acetylation (Ac-VVIA) or amidation (VVIA-NH_2), respectively, on Y fluorescence of Aβ42 and its Y-substituted analogues. Representative spectra are shown in Supplementary Fig. S2. The results are shown in the third and fourth bars of each group in Fig. 3D, respectively. Upon addition of Ac-VVIA or VVIA-NH_2, the fluorescence of [Y1]Aβ42 increased by 48 ± 3% and 62 ± 6%, respectively. These values were 2.4- and 1.8-times lower than with unmodified Aβ(39–42), suggesting that both the carboxyl and amino groups of Aβ(39–42) contributed to the interaction with Aβ42. The larger loss of affinity caused by blocking the N-terminus relative to blocking the C-terminus of Aβ(39–42) is consistent with the loss of inhibitory activity observed for the N-terminally acetylated analogue (Fig. 1). Small effects on fluorescence were observed in two other positions. The fluorescence of Aβ42 decreased by 19 ± 3% upon addition of Ac-VVIA and the fluorescence of [Y30]Aβ42 decreased by 24 ± 3% upon addition of VVIA-NH_2. These data suggested that removing either one of the charges in Aβ(39–42) decreased the affinity of the peptide for the putative Aβ42 N-terminal binding site and increased affinity for alternative binding sites.

Analysis of the interaction of other Aβ(39–42) analogues with [Y1]Aβ42 using internal Y fluorescence showed that the fluorescence increase induced by the N-terminally acetylated and C-terminally amidated retro sequences (Ac-AIVV and AIVV-NH_2), and by the inverso-peptide (vvia) also were significantly lower than those of Aβ(39–42) (Fig. S3), in agreement with the low inhibitory activity of these analogues. Not all the fluorescence results

correlated directly with the inhibition data presented in Fig.1, presumably because small sequence perturbation might affect the binding mode of the tetrapeptide derivatives. Exploring the binding sites of all the derivatives was beyond the scope of this study, which was limited to delineation of the major binding sites of the lead compound and the effect of the structural changes that were found to have the greatest effect on the inhibitory activity, namely, the charge and chirality in Aβ(39–42) analogues, which also had the greatest effect on binding to the N-terminal region of Aβ42.

Solution-state NMR characterization of the interaction between Aβ(39–42) and Aβ42—To complement the intrinsic fluorescence experiments, we used solution-state, $^{15}N–^{1}H$ and $^{13}C–^{1}H$ heteronulear single quantum coherence (HSQC) NMR experiments, which enable detection of residue-specific signal perturbation upon binding of unlabeled Aβ(39–42) to ^{15}N- or $^{13}C/^{15}N$-labeled Aβ42. In preliminary experiments, the NMR signal was observed to decrease gradually over 24 h due to self-assembly of Aβ42, as reported previously.[39] Nonetheless, during the relatively short time needed for acquiring HSQC spectra (~37 min), perturbation of specific resonances upon addition of Aβ(39–42) could be observed.

The chemical shifts of most of the amino acid residues in Aβ42 remained unchanged in the presence of 8-fold molar excess Aβ(39–42) with the exceptions of small changes in D and R side chains. 2D $H^{\beta}(C^{\beta})CO$ experiments optimized to detect D side chains were collected to identify and monitor the interaction of these side chains with Aβ(39–42). As shown in Fig. 4A, the $^{1}H/^{13}C$ signal of the D7 and D23 side-chains showed a small shift and decreased in intensity upon addition of Aβ(39–42) to Aβ42. The resonances for the D1 side chain were isolated from D7 and D23 side-chain resonances and appeared as multiple cross-peaks likely due to slow chemical exchange. The side-chain resonance of R5 also was perturbed upon addition of Aβ(39–42) to Aβ42 as shown by a small upfield shift and decreased intensity of the N^{ε}-H^{ε} crosspeak in $^{15}N–^{1}H$ HSQC (Fig. 4B). The data suggested that Aβ(39–42) bound weakly, yet specifically to Aβ42 at positions near the charged residues D1, R5, and D7 at the N-terminus, as well as near D23.

To further explore the binding, we studied the interaction of two analogues that showed weak or moderate inhibition of Aβ42-induced toxicity (Fig. 1) and increase in [Y1]Aβ42 fluorescence (Figs. 3D and S3), Ac-VVIA and vvia, in NMR binding experiment. The chemical shift changes of D1, D7 and D23 found upon addition of Ac-VVIA (Fig. S4) and vvia (inverso-peptide) (Fig. S5) were small, similar to those induced by VVIA. These results were consistent with the toxicity inhibition and intrinsic fluorescence data, but the small magnitude of the effects observed in the NMR experiments did not allow drawing further conclusions regarding the binding site(s) of the tetrapeptide derivatives on Aβ42.

Discussion and Conclusions

Aβ(39–42) is a promising inhibitor of Aβ42-induced toxicity, which unlike most peptide-based drug leads, has favorable physicochemical characteristics. For future development of this peptide lead towards metabolically stable peptidomimetic derivatives, a detailed understanding of its mechanism of action is needed. Here, using a combination of cell cultural and biophysical methods, we found that the major mechanism by which Aβ(39–42) inhibits Aβ42-induced toxicity is through specific interaction with Aβ42, in agreement with computer modeling predictions,[25] DLS[23,24] and ion-mobility-spectroscopy–mass-spectrometry findings.[40] In addition, Aβ(39–42) showed a weak, non-specific protective effect. Interestingly, contrary to our initial hypothesis, the binding of Aβ(39–42) appears to occur predominantly at the N-terminus of Aβ42.

Determination of the binding site of compounds that inhibit Aβ assembly and toxicity is challenging because of the difficulties associated with high-resolution structural study of Aβ itself. Co-crystals of Aβ with inhibitors are difficult to obtain and the metastable character of Aβ oligomers does not lend itself easily to high-resolution structure determination. The combination of our SAR (Fig. 1), fluorescence (Fig. 3), and NMR (Fig. 4) data, and the weak effect of Aβ(39–42) on alamethicine- or α-synuclein-induced toxicity (Fig. 2) all suggest that Aβ(39–42) binds to Aβ42 specifically, predominantly at the N-terminus.

Multiple findings support an important role for the N-terminus of Aβ in mediating assembly and toxicity. Two familial AD-linked mutations resulting in the English (H6R)[41] and Tottori (D7N)[42] variants were found to stabilize ordered secondary structural elements in Aβ monomers, facilitate Aβ oligomerization, and produce oligomeric assemblies that larger and are more toxic than those of WT Aβ.[43] In addition, a double substitution of the first two N-terminal residues of Aβ, D1E/A2V, increases protofibril formation substantially.[44] Thus, the N-terminal region plays and important role in Aβ assembly and toxicity suggesting that small molecule binding in this region may inhibit Aβ toxicity. In addition, N-terminally truncated Aβ analogues, particularly those containing an N-terminal pyroglutamate (pE), e.g., [pE3]Aβ or [pE11]Aβ, were found in senile plaques and have been reported to form β-sheet faster and with higher propensity,[45,46] and to be more toxic than WT Aβ.[47,48] One mechanism by which Aβ(39–42) may reduce Aβ42 toxicity is by masking putative enzymatic cleavage sites and thereby preventing the truncation of the N-terminus.

The observation that the N-terminally-acetylated Aβ(39–42) analogues, Ac-VVIA and Ac-AIVV, did not inhibit Aβ42-induced toxicity suggests that electrostatic interactions between the unprotected, positively charged N-terminal amino group of Aβ(39–42) and negatively charged side-chain groups in Aβ42 might be important for inhibitory activity. The observation of small chemical shift changes in the resonances of D1 and D7, but not E3, (Fig. 4A), supports the specificity of the binding. An alternative explanation for the lack of inhibition by the acetylated peptides may be creation of specific degradation signals (degrons),[49] leading to rapid proteolysis of Ac-VVIA and Ac-AIVV. However, the large difference between the perturbation of the intrinsic fluorescence of [Y1]Aβ42 by free and acetylated analogues (Figs. 3D and S3) supports an important role for Coulombic interaction involving the amino group of Aβ(39–42) and negatively charged side chains in the N-terminus of Aβ42, and suggest that degradation is unlikely the reason for the low inhibition by the acetylated analogues. The observations that amidation of the C-terminus also lowered perturbation of [Y1]Aβ42 fluorescence (Fig. 3D) and of a chemical shift and intensity change in the resonance of R5 (Fig. 4B) provide additional support for contribution of specific electrostatic interactions between Aβ(39–42) and the N-terminal region of Aβ42.

In addition to the electrostatic interactions found here, modeling studies have suggested that the hydrophobic residues A2 and F4 are important for interaction of Aβ with cellular membranes and potential inhibitors.[25,50] Our data also support an amphiphilic character for the interaction between Aβ(39–42) and the N-terminus of Aβ42. Thus, the SAR experiments (Fig. 1) show that both the hydrophobic side chain at position 41 and the charged N-terminal amino group are important for inhibitory activity.

The C-terminus of Aβ42 is predicted to be shielded to a large extent from the aqueous milieu in Aβ oligomers, a prediction supported by multiple studies,[6–8,10,51] and by the high fluorescence of the Y residues in [Y30]Aβ42 and [Y42]Aβ42 (Fig. 3C). Thus, the observation that the fluorescence of [Y30]Aβ42 and [Y42]Aβ42 did not change significantly upon addition of Aβ(39–42) may result from lower accessibility of the C-terminal region of Aβ42 to the tetrapeptide. Alternatively, Aβ(39–42) may bind the C-terminus without causing substantial change in Y fluorescence because the overall hydrophobicity in the

vicinity of the Y side-chain does not change significantly. However, we did not observe any perturbation of NMR resonances in the C-terminal region of Aβ42 in the presence of 8-fold molar excess Aβ(39–42) suggesting low probability of binding of the tetrapeptide in this region.

Notably, we observed an increase in the fluorescence emission of Aβ42 analogues and their mixtures with tetrapeptides in wavelengths longer than the Y emission window (Fig. S2). This increase in emission likely is due to light scattering and presumably reflects promotion of Aβ42 assembly by the tetrapeptides, as we observed previously in DLS experiments.[23,24]

Though further work will be required to elucidate the exact binding mode of Aβ(39–42) to Aβ42, our data demonstrate the specificity of this tetrapeptide as an inhibitor of Aβ42-induced toxicity and shed light on the mechanism by which Aβ(39–42) binds to Aβ42 and blocks its toxicity. The current study provides structural basis for future development of effective and stable peptidomimetic inhibitors of Aβ42 neurotoxicity as potential AD therapeutics.

Experimental Section

Chemicals and Reagents

9-Fluorenylmethoxycarbonyl (FMOC)-protected amino acids and NovaSyn TGA resin were purchased from Novabiochem (Gibbstown, NJ). Wang and PAL resins and all other reagents were obtained from Sigma-Aldrich (St. Louis, MO) and were of the highest purity available. High-purity water (18.2 MΩ) was obtained using a Milli-Q system (Millipore, Bedford, MA).

Peptide Synthesis

Synthesis, purification, and characterization of Aβ42 and Aβ42 analogues with Y substituted at positions 1, 20, 30, and 42 and F substituted at position 10 were carried out as described previously,[34] purified using reverse-phase high-performance liquid chromatography (RP-HPLC), and characterized by MS and amino acid analysis (AAA).

Aβ(39–42) and its derivatives were synthesized using a Discover® microwave-assisted synthesis system (CEM, Matthews, NC) using the following general protocol: FMOC-protected, pre-loaded NovaSyn TGA resin or PAL resin (0.1 mmol) was placed in a peptide synthesis vessel, swollen in *N*,*N*-dimethylformamide (DMF), and deprotected with 5 mL of 20% piperidine (or 4-methylpiperidine) in DMF for 20 min at room temperature. After washing with DMF thrice, a mixed solution of 0.3 mmol FMOC-AA-OH, 0.3 mmol 2-(1H-benzotriazole-1-yl)-1,1,3,3-tetramethyluronium hexafluorophosphate, and 0.6 mmol *N*,*N*-diisopropylethylamine in 4 mL DMF was added to the reaction vessel. The coupling reaction was performed using 40 W microwave energy for 8 min at 50°C. 2,4,6-Trinitrobenzenesulfonic acid test was applied to check for remaining free amino groups.[52] Coupling efficiency was monitored by the formation of piperidine-dibenzofulvene or 4-methylpiperidine-dibenzofulvene using UV spectroscopy.[53,54] Acetylation of the N-terminus of Ac-VVIA and Ac-AIVV was performed using acetic anhydride/pyridine (1:2 v/v). After completion of the sequence, the resin was thoroughly washed with DMF and then with dichloromethane, dried under vacuum and the peptide was cleaved using a mixture of trifluoroacetic acid/1,2-ethanedithiol/H_2O (95:2.5:2.5). Peptides were precipitated by addition of cold diethyl ether and purified by RP-HPLC. The purity of all peptides was higher than 95% determined by analytical RP-HPLC. Peptides were further characterized by MS and AAA. The peptide sequences, calculated masses, and observed masses are listed in Table 2.

Cell Viability Assays

The methods for evaluation of the biological activity of the CTFs themselves and their inhibition of Aβ42-induced toxicity were described previously.[23] Briefly, PC-12 cells were differentiated into a neuronal phenotype by incubation with nerve growth factor (100 ng/mL) for 48 h. For initial screening of the new analogues, the cells then were incubated with solutions of Aβ42 alone at 10 μM nominal concentration, Aβ(39–42) analogues alone at 100 μM nominal concentration, or Aβ42:Aβ(39–42) analogue mixtures at 1:10 concentration ratio, respectively, for 24 h. Cell viability was determined by the MTT assay using a CellTiter 96® kit (Promega, Madison, WI). Negative controls included NaOH at the same concentration as in the peptide solutions and medium alone. A positive control was 1 μM staurosporine for full kill, which was used to represent a 100% reduction in cell viability, based on which the percentage viability of all of the experimental conditions was calculated. Active analogues were characterized further in dose–response experiments. In these experiments, Aβ42 alone and Aβ42:Aβ(39–42) analogue mixtures at 1:1, 1:2, 1:5, and 1:10 concentration ratios were used and cell viability was determined by both the MTT assay and the LDH-release assay (CytoTox-ONE Homogenous Membrane Integrity Assay kit (Promega)). At least three independent experiments with six replicates ($n \geq 18$) were performed for each assay. The results were averaged and presented as mean ± SEM. Dose–response assays for inhibition of staurosporine-, α-synuclein-, or alamethicin-induced toxicity by Aβ(39–42) were performed using a similar protocol.

Intrinsic Fluorescence

Aβ42 or its Y-substituted analogues in the absence or presence of Aβ(39–42) or its analogues were treated with HFIP as described previously.[55] Dry, HFIP-treated peptide films were dissolved in 60 mM NaOH at 10% of the final volume and then diluted with 10 mM sodium phosphate, pH 7.4, to the final nominal concentrations, Aβ42 at 5 μM and Aβ(39–42) or its analogues at 50 μM. Samples were centrifuged at 5,000 *g* for 1 min to remove trace amount of dust particles that could interfere with the experiment due to light scattering. The exact concentration was determined *post facto* by AAA. Fluorescence was measured using a Hitachi F4500 spectrofluorimeter (Hitachi Instruments, Rye, NH) with excitation at 280 nm and emission in the range 290–400 nm. At least 10 measurements of ~1 min each were taken immediately following sample preparation. All fluorescence measurements were carried out at 22°C with a scan rate of 240 nm/min. Slit widths used for excitation and emission were 5 and 10 nm, respectively. The fluorescence emission spectrum of the phosphate buffer (background intensity) was subtracted from the emission spectrum of each sample. The area under the curve was calculated and normalized as the fluorescence intensity per micromole. Four independent experiments were carried out. The results were averaged and are presented as mean ± SEM of fluorescence intensity (arbitrary units) or percentage of the fluorescence intensity of control peptides.

Electron Microscopy

Morphological examination was performed as described briefly.[56] Briefly, aliquots of each Aβ42 analogue in the absence or presence of Aβ(39–42) or its analogues were spotted on glow-discharged, carbon-coated Formvar grids (Electron Microscopy Science, Hatfield, PA). The samples were the same as those used in the fluorescence experiments. Samples were incubated for 10 min, fixed with 5 μL 2.5% glutaraldehyde for 10 min, and stained with 5 μL 1% uranyl acetate for 10 min. Three to six replicates of each peptide were analyzed using a CX 100 transmission electron microscope (JEOL, Peabody, MA).

Solution-state NMR

Uniformly isotopically labeled Aβ42 ([^{15}N] or [^{13}C/^{15}N]) were purchased from rPeptide (Athens, GA) and treated with HFIP to disaggregate pre-existing aggregates as described previously.[55] The peptide was dissolved in 20 mM potassium phosphate, pH 7.2, at nominal concentration 1 mg/mL and then sonicated for 1 min. Aβ(39–42) was dissolved in 10 mM NaOH at 2 mg/mL and sonicated for 1 min. Then, Aβ42 and Aβ(39–42) were mixed slowly to final concentrations 32 μM and 256 μM, respectively (1:8 concentration ratio). A control ^{15}N-Aβ42 sample at 32 μM was prepared by adding the same proportion of buffer and NaOH in the absence of Aβ(39–42) to the Aβ42 stock solution to match the solvent concentration and pH. 2D ^{15}N–^{1}H HSQC NMR spectra of freshly prepared ^{15}N-labeled Aβ42 samples in the absence or presence of Aβ(39–42) were collected at 4 °C using a 600 MHz Bruker Avance II spectrometer equipped with a cryoprobe. The acquisition time was ~37 min for each HSQC spectrum. The average intensity percentage of the five strongest, unequivocally assigned peaks in Aβ42 (Y10, V18, A21, I32, and L34) was used to calculate the relative Aβ42 monomer concentration. $H^{\beta}(C^{\beta})CO$ experiments were collected to support aspartate assignments in Aβ42 and to monitor Aβ42 and Aβ(39–42) interactions.

Supplementary Material

Refer to Web version on PubMed Central for supplementary material.

Acknowledgments

We thank Dr. David Teplow for the use of his spectrofluorometer and plate reader and Drs. Brigita Urbanc, Dahabada Lopes, Raz Jelinek, Farid Rahimi, Inna Solomonov, and Panchanan Maiti for critical reading of the manuscript and helpful discussions. The work was supported by grant AG027818 from the NIH/NIA.

Glossary

AAA	amino acid analysis
Aβ	amyloid β-protein
AD	Alzheimer's disease
CHC	central hydrophobic cluster
CTF	C-terminal fragment
DMF	*N*,*N*,-dimethylformamide
EM	electron microscopy,
FMOC	9-fluorenylmethoxycarbonyl
HFIP	1,1,1,3,3,3-hexafluoroisopropanol
HSQC	heteronulear single quantum coherence
LDH	lactate dehydrogenase
MTT	(3-(4,5-dimethylthiazol-2-yl)-2,5-diphenyltetrazolium bromide
MS	mass spectrometry
RP-HPLC	reverse-phase high-performance liquid chromatography
SAR	structure–activity relationship
ST	staurosporine
tPSA	topological polar surface area

WT wild-type

References

1. Walsh DM, Selkoe DJ. Aβ oligomers - a decade of discovery. J Neurochem. 2007; 101:1172–1184. [PubMed: 17286590]
2. Kirkitadze MD, Bitan G, Teplow DB. Paradigm shifts in Alzheimer's disease and other neurodegenerative disorders: The emerging role of oligomeric assemblies. J Neurosci Res. 2002; 69:567–577. [PubMed: 12210822]
3. Hardy J, Selkoe DJ. The amyloid hypothesis of Alzheimer's disease: progress and problems on the road to therapeutics. Science. 2002; 297:353–356. [PubMed: 12130773]
4. Ferreira ST, Vieira MN, De Felice FG. Soluble protein oligomers as emerging toxins in alzheimer's and other amyloid diseases. IUBMB Life. 2007; 59:332–345. [PubMed: 17505973]
5. Dahlgren KN, Manelli AM, Stine WB Jr, Baker LK, Krafft GA, LaDu MJ. Oligomeric fibrillar species of amyloid-β peptides differentially affect neuronal viability. J Biol Chem. 2002; 277:32046–32053. [PubMed: 12058030]
6. Bitan G, Kirkitadze MD, Lomakin A, Vollers SS, Benedek GB, Teplow DB. Amyloid β-protein (Aβ) assembly: Aβ40 and Aβ42 oligomerize through distinct pathways. Proc Natl Acad Sci USA. 2003; 100:330–335. [PubMed: 12506200]
7. Bernstein SL, Dupuis NF, Lazo ND, Wyttenbach T, Condron MM, Bitan G, Teplow DB, Shea JE, Ruotolo BT, Robinson CV, Bowers MT. Amyloid-β protein oligomerization and the importance of tetramers and dodecamers in the aetiology of Alzheimer's disease. Nat Chem. 2009; 1:326–331. [PubMed: 20703363]
8. Bitan G, Vollers SS, Teplow DB. Elucidation of primary structure elements controlling early amyloid β-protein oligomerization. J Biol Chem. 2003; 278:34882–34889. [PubMed: 12840029]
9. Lazo ND, Grant MA, Condron MC, Rigby AC, Teplow DB. On the nucleation of amyloid β-protein monomer folding. Protein Sci. 2005; 14:1581–1596. [PubMed: 15930005]
10. Urbanc B, Cruz L, Yun S, Buldyrev SV, Bitan G, Teplow DB, Stanley HE. *In silico* study of amyloid β-protein folding and oligomerization. Proc Natl Acad Sci USA. 2004; 101:17345–17350. [PubMed: 15583128]
11. Tjernberg LO, Näslund J, Lindqvist F, Johansson J, Karlstrom AR, Thyberg J, Terenius L, Nordstedt C. Arrest of β-amyloid fibril formation by a pentapeptide ligand. J Biol Chem. 1996; 271:8545–8548. [PubMed: 8621479]
12. Soto C, Kindy MS, Baumann M, Frangione B. Inhibition of Alzheimer's amyloidosis by peptides that prevent β-sheet conformation. Biochem Biophys Res Commun. 1996; 226:672–680. [PubMed: 8831674]
13. Lowe TL, Strzelec A, Kiessling LL, Murphy RM. Structure-function relationships for inhibitors of β-amyloid toxicity containing the recognition sequence KLVFF. Biochemistry. 2001; 40:7882–7889. [PubMed: 11425316]
14. Findeis MA, Musso GM, Arico-Muendel CC, Benjamin HW, Hundal AM, Lee JJ, Chin J, Kelley M, Wakefield J, Hayward NJ, Molineaux SM. Modified-peptide inhibitors of amyloid β-peptide polymerization. Biochemistry. 1999; 38:6791–6800. [PubMed: 10346900]
15. Hughes E, Burke RM, Doig AJ. Inhibition of toxicity in the β-amyloid peptide fragment β-(25–35) using N-methylated derivatives - A general strategy to prevent amyloid formation. J Biol Chem. 2000; 275:25109–25115. [PubMed: 10825171]
16. Gordon DJ, Sciarretta KL, Meredith SC. Inhibition of β-amyloid(40) fibrillogenesis and disassembly of β-amyloid(40) fibrils by short β-amyloid congeners containing N-methyl amino acids at alternate residues. Biochemistry. 2001; 40:8237–8245. [PubMed: 11444969]
17. Zhang S, Iwata K, Lachenmann MJ, Peng JW, Li S, Stimson ER, Lu Y, Felix AM, Maggio JE, Lee JP. The Alzheimer's peptide Aβ adopts a collapsed coil structure in water. J Struct Biol. 2000; 130:130–141. [PubMed: 10940221]

18. Hochdörffer K, März-Berberich J, Nagel-Steger L, Epple M, Meyer-Zaika W, Horn AH, Sticht H, Sinha S, Bitan G, Schrader T. Rational design of β-Sheet ligands against $A\beta_{42}$-induced toxicity. J Am Chem Soc. 2011; 133:4348–4358. [PubMed: 21381732]
19. Hetenyi C, Szabo Z, Klement T, Datki Z, Kortvelyesi T, Zarandi M, Penke B. Pentapeptide amides interfere with the aggregation of β-amyloid peptide of Alzheimer's disease. Biochem Biophys Res Commun. 2002; 292:931–936. [PubMed: 11944904]
20. Szegedi V, Fülöp L, Farkas T, Rozsa E, Robotka H, Kis Z, Penke Z, Horvath S, Molnar Z, Datki Z, Soos K, Toldi J, Budai D, Zarandi M, Penke B. Pentapeptides derived from Aβ1–42 protect neurons from the modulatory effect of Aβ fibrils—an in vitro and in vivo electrophysiological study. Neurobiol Dis. 2005; 18:499–508. [PubMed: 15755677]
21. Pratim Bose P, Chatterjee U, Nerelius C, Govender T, Norstrom T, Gogoll A, Sandegren A, Gothelid E, Johansson J, Arvidsson PI. Poly-N-methylated amyloid β-peptide (Aβ) C-terminal fragments reduce Aβ toxicity in vitro and in Drosophila melanogaster. J Med Chem. 2009; 52:8002–8009. [PubMed: 19908889]
22. Rahimi AF, Shanmugam A, Bitan G. Structure–function relationships of pre-fibrillar protein assemblies in Alzheimer's disease and related disorders. Curr Alzheimer Res. 2008; 5:319–341. [PubMed: 18537546]
23. Fradinger EA, Monien BH, Urbanc B, Lomakin A, Tan M, Li H, Spring SM, Condron MM, Cruz L, Xie CW, Benedek GB, Bitan G. C-terminal peptides coassemble into Aβ42 oligomers and protect neurons against Aβ42-induced neurotoxicity. Proc Natl Acad Sci USA. 2008; 105:14175–14180. [PubMed: 18779585]
24. Li H, Monien BH, Lomakin A, Zemel R, Fradinger EA, Tan M, Spring SM, Urbanc B, Xie CW, Benedek GB, Bitan G. Mechanistic investigation of the inhibition of Aβ42 assembly and neurotoxicity by Aβ42 C-terminal fragments. Biochemistry. 2010; 49:6358–6364. [PubMed: 20568734]
25. Urbanc B, Betnel M, Cruz L, Li H, Fradinger EA, Monien BH, Bitan G. Structural basis for Aβ(1–42) toxicity inhibition by Aβ C-terminal fragments: discrete molecular dynamics study. J Mol Biol. 2011; 410:316–328. [PubMed: 21621545]
26. Lipinski CA, Lombardo F, Dominy BW, Feeney PJ. Experimental and computational approaches to estimate solubility and permeability in drug discovery and development settings. Adv Drug Del Rev. 2001; 46:3–26.
27. Veber DF, Johnson SR, Cheng HY, Smith BR, Ward KW, Kopple KD. Molecular properties that influence the oral bioavailability of drug candidates. J Med Chem. 2002; 45:2615–2623. [PubMed: 12036371]
28. Bertrand R, Solary E, O'Connor P, Kohn KW, Pommier Y. Induction of a common pathway of apoptosis by staurosporine. Exp Cell Res. 1994; 211:314–321. [PubMed: 8143779]
29. Arispe N, Diaz JC, Simakova O. Aβ ion channels. Prospects for treating Alzheimer's disease with Aβ channel blockers. Biochim Biophys Acta. 2007; 1768:1952–1965. [PubMed: 17490607]
30. Sokolov Y, Kozak JA, Kayed R, Chanturiya A, Glabe C, Hall JE. Soluble amyloid oligomers increase bilayer conductance by altering dielectric structure. J Gen Physiol. 2006; 128:637–647. [PubMed: 17101816]
31. Fringeli UP, Fringeli M. Pore formation in lipid membranes by alamethicin. Proc Natl Acad Sci USA. 1979; 76:3852–3856. [PubMed: 291045]
32. Auluck PK, Caraveo G, Lindquist S. α-Synuclein: membrane interactions and toxicity in Parkinson's disease. Annu Rev Cell Dev Biol. 2010; 26:211–233. [PubMed: 20500090]
33. Condron MM, Monien BH, Bitan G. Synthesis and purification of highly hydrophobic peptides derived from the C-terminus of amyloid β-protein. Open Biotechnol J. 2008; 2:87–93. [PubMed: 19898686]
34. Maji SK, Amsden JJ, Rothschild KJ, Condron MM, Teplow DB. Conformational dynamics of amyloid β-protein assembly probed using intrinsic fluorescence. Biochemistry. 2005; 44:13365–13376. [PubMed: 16201761]
35. Maji SK, Ogorzalek Loo RR, Inayathullah M, Spring SM, Vollers SS, Condron MM, Bitan G, Loo JA, Teplow DB. Amino acid position-specific contributions to amyloid β-protein oligomerization. J Biol Chem. 2009; 284:23580–23591. [PubMed: 19567875]

36. Lakowicz, JR. Principles of fluorescence spectroscopy. 2. Kluwer Academic/Plenum Publishers; New York: 1999. p. 698
37. Zagorski MG, Yang J, Shao H, Ma K, Zeng H, Hong A. Methodological and chemical factors affecting amyloid β peptide amyloidogenicity. Methods Enzymol. 1999; 309:189–204. [PubMed: 10507025]
38. Stine WB Jr, Dahlgren KN, Krafft GA, LaDu MJ. In vitro characterization of conditions for amyloid-β peptide oligomerization fibrillogenesis. J Biol Chem. 2003; 278:11612–11622. [PubMed: 12499373]
39. Yan Y, Wang C. Aβ42 is more rigid than Aβ40 at the C terminus: implications for Aβ aggregation and toxicity. J Mol Biol. 2006; 364:853–862. [PubMed: 17046788]
40. Gessel MM, Wu C, Li H, Bitan G, Shea JE, Bowers MT. Unpublished results.
41. Janssen JC, Beck JA, Campbell TA, Dickinson A, Fox NC, Harvey RJ, Houlden H, Rossor MN, Collinge J. Early onset familial Alzheimer's disease - Mutation frequency in 31 families. Neurology. 2003; 60:235–239. [PubMed: 12552037]
42. Wakutani Y, Watanabe K, Adachi Y, Wada-Isoe K, Urakami K, Ninomiya H, Saido TC, Hashimoto T, Iwatsubo T, Nakashima K. Novel amyloid precursor protein gene missense mutation (D678N) in probable familial Alzheimer's disease. J Neurol Neurosurg Psychiatry. 2004; 75:1039–1042. [PubMed: 15201367]
43. Ono K, Condron MM, Teplow DB. Effects of the English (H6R) and Tottori (D7N) familial Alzheimer disease mutations on amyloid β-protein assembly and toxicity. J Biol Chem. 2010; 285:23186–23197. [PubMed: 20452980]
44. Qahwash I, Weiland KL, Lu YF, Sarver RW, Kletzien RF, Yan RQ. Identification of a mutant amyloid peptide that predominantly forms neurotoxic protofibrillar aggregates. J Biol Chem. 2003; 278:23187–23195. [PubMed: 12684519]
45. He WL, Barrow CJ. The A β 3-pyroglutamyl and 11-pyroglutamyl peptides found in senile plaque have greater β-sheet forming and aggregation propensities in vitro than full-length A β. Biochemistry. 1999; 38:10871–10877. [PubMed: 10451383]
46. Schilling S, Lauber T, Schaupp M, Manhart S, Scheel E, Bohm G, Demuth HU. On the seeding and oligomerization of pGlu-amyloid peptides (in vitro). Biochemistry. 2006; 45:12393–12399. [PubMed: 17029395]
47. Russo C, Violani E, Salis S, Venezia V, Dolcini V, Damonte G, Benatti U, D'Arrigo C, Patrone E, Carlo P, Schettini G. Pyroglutamate-modified amyloid β-peptides - A β N3(pE)-strongly affect cultured neuron and astrocyte survival. J Neurochem. 2002; 82:1480–1489. [PubMed: 12354296]
48. Wirths O, Breyhan H, Cynis H, Schilling S, Demuth HU, Bayer TA. Intraneuronal pyroglutamate-Aβ 3–42 triggers neurodegeneration and lethal neurological deficits in a transgenic mouse model. Acta Neuropathol. 2009; 118:487–496. [PubMed: 19547991]
49. Hwang CS, Shemorry A, Varshavsky A. N-terminal acetylation of cellular proteins creates specific degradation signals. Science. 2010; 327:973–977. [PubMed: 20110468]
50. Urbanc B, Betnel M, Cruz L, Bitan G, Teplow DB. Elucidation of amyloid β-protein oligomerization mechanisms: discrete molecular dynamics study. J Am Chem Soc. 2010; 132:4266–4280. [PubMed: 20218566]
51. Zhao WQ, Toolan D, Hepler RW, Wolfe AL, Yu Y, Price E, Uebele VN, Schachter JB, Reynolds IJ, Renger JJ, McCampbell A, Ray WJ. High throughput monitoring of amyloid-β42 assembly into soluble oligomers achieved by sensitive conformation state-dependent immunoassays. J Alzheimers Dis. 2011; 25:655–669. [PubMed: 21483096]
52. Chan, WC.; White, PD. Fmoc solid phase peptide synthesis : a practical approach. Oxford University Press; New York: 2000. p. xxivp. 346
53. Gude M, Ryf J, White PD. An accurate method for the quantitiation of Fmoc-derivatized solid phase support. Lett Pept Sci. 2002; 9:203–206.
54. Varady L, Rajur SB, Nicewonger RB, Guo M, Ditto L. Fast and quantitative high-performance liquid chromatography method for the determination of 9-fluorenylmethoxycarbonyl release from solid-phase synthesis resins. J Chromatogr A. 2000; 869:171–179. [PubMed: 10720236]

55. Rahimi, F.; Maiti, P.; Bitan, G. Photo-induced cross-linking of unmodified proteins (PICUP) applied to amyloidogenic peptides. J Vis Exp. 2009. http://www.jove.com/index/details.stp?id=1071

56. Li H, Monien BH, Fradinger EA, Urbanc B, Bitan G. Biophysical characterization of Aβ42 C-terminal fragments: inhibitors of Aβ42 neurotoxicity. Biochemistry. 2010; 49:1259–1267. [PubMed: 20050679]

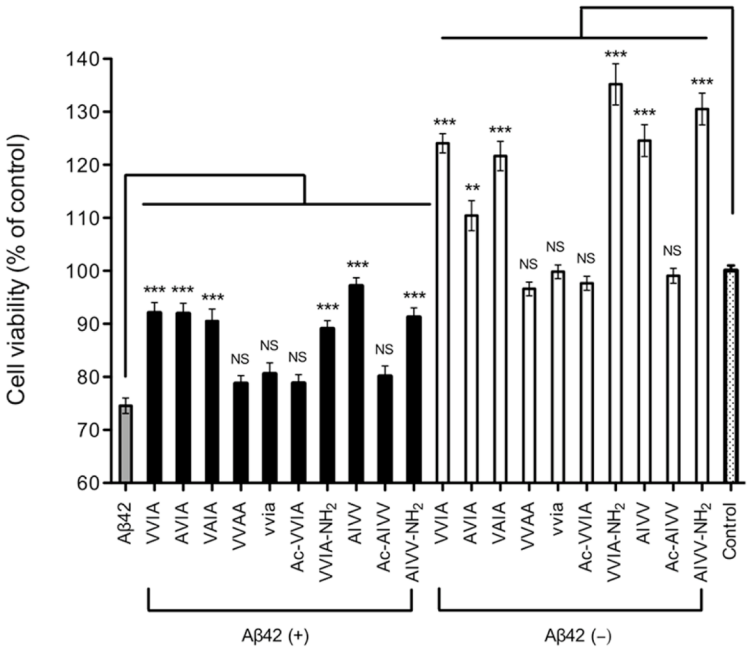

Figure 1. Evaluation of inhibitory activity of Aβ(39–42) analogues

Aβ42 (10 μM, grey bar), mixtures of Aβ42: Aβ(39–42) analogues at 1:10 concentration ratio (black bars), Aβ(39–42) analogues alone at 100 μM (white bars), or control medium containing NaOH at the same concentration as in the peptide solutions (dotted bar) were incubated with differentiated PC-12 cells for 24 h and cell viability was measured using the MTT assay. The data are shown as mean ± SEM of at least three independent experiments with 6 replicates per data point ($n \geq 18$). Statistical significance was calculated and compared with Aβ42 alone by using ANOVA followed by Dennett's multiple-comparison tests (**$p < 0.01$, ***$p < 0.001$).

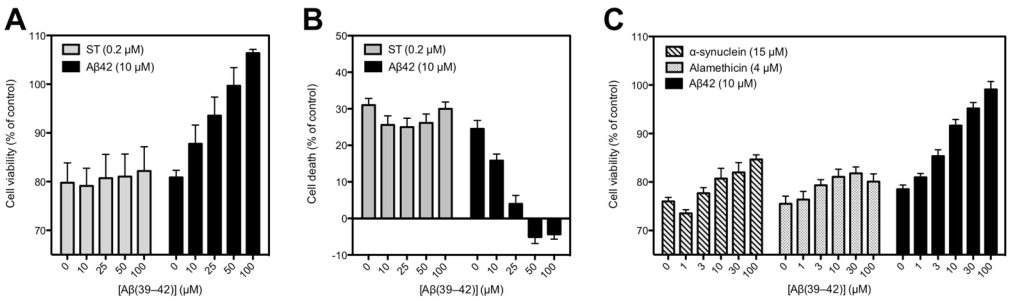

Figure 2. Aβ(39–42) selectively inhibits Aβ42-induced toxicity

Aβ42 (10 μM) or staurosporine (ST, 0.2 μM) in the absence or presence of different Aβ(39–42) concentrations were A) incubated with differentiated PC-12 cells for 24 h and cell viability was determined using MTT assay; and B) incubated with differentiated PC-12 cells for 48 h and cell death was measured using LDH assay. C) α-synuclein (15 μM), alamethicin (4 μM), or Aβ42 (10 μM) in the absence or presence of different Aβ(39–42) concentrations were incubated with differentiated PC-12 cells for 24 h and viability was determined using MTT assay. The data represent mean ± SEM from at least three independent experiments with 5 replicates per data point (n ≥ 15).

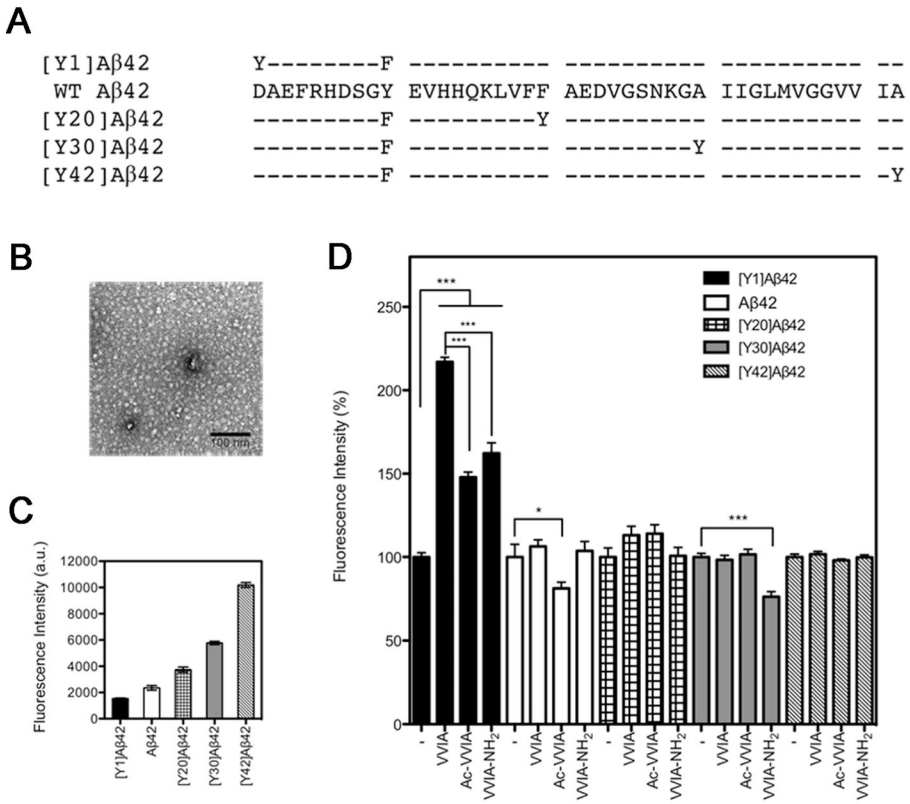

Figure 3. Intrinsic fluorescence of Aβ42 analogues in the presence of Aβ(39–42) or its derivatives

A) Primary structure of Aβ42 and its Y-substituted analogues. Hyphens indicate residues identical to WT Aβ42. In WT Aβ42, Y is at position 10. The substitutions, in which a single Y residue substituted the original residues at positions (n) 1, 20, 30, or 42, and the native Y10 was substituted by F, are simply named [Yn]Aβ42. B) Representative electron micrograph of freshly prepared 5 μM Aβ42. The scale bar represents 100 nm. C) Intrinsic fluorescence intensity of 5 μM Aβ42 and each Y-substituted analogue. D) Intrinsic fluorescence of Aβ42 analogues in the presence of Aβ(39–42), Ac-VVIA, or VVIA-NH_2 normalized to the percentage of each Aβ42 analogue alone. The data are shown as mean ± SEM of 4 independent experiments with at least 10 measurements per data point. Statistical significance was analyzed using ANOVA followed by Bonferroni's and Dennett's multiple-comparison tests (*$p < 0.05$, ***$p < 0.001$).

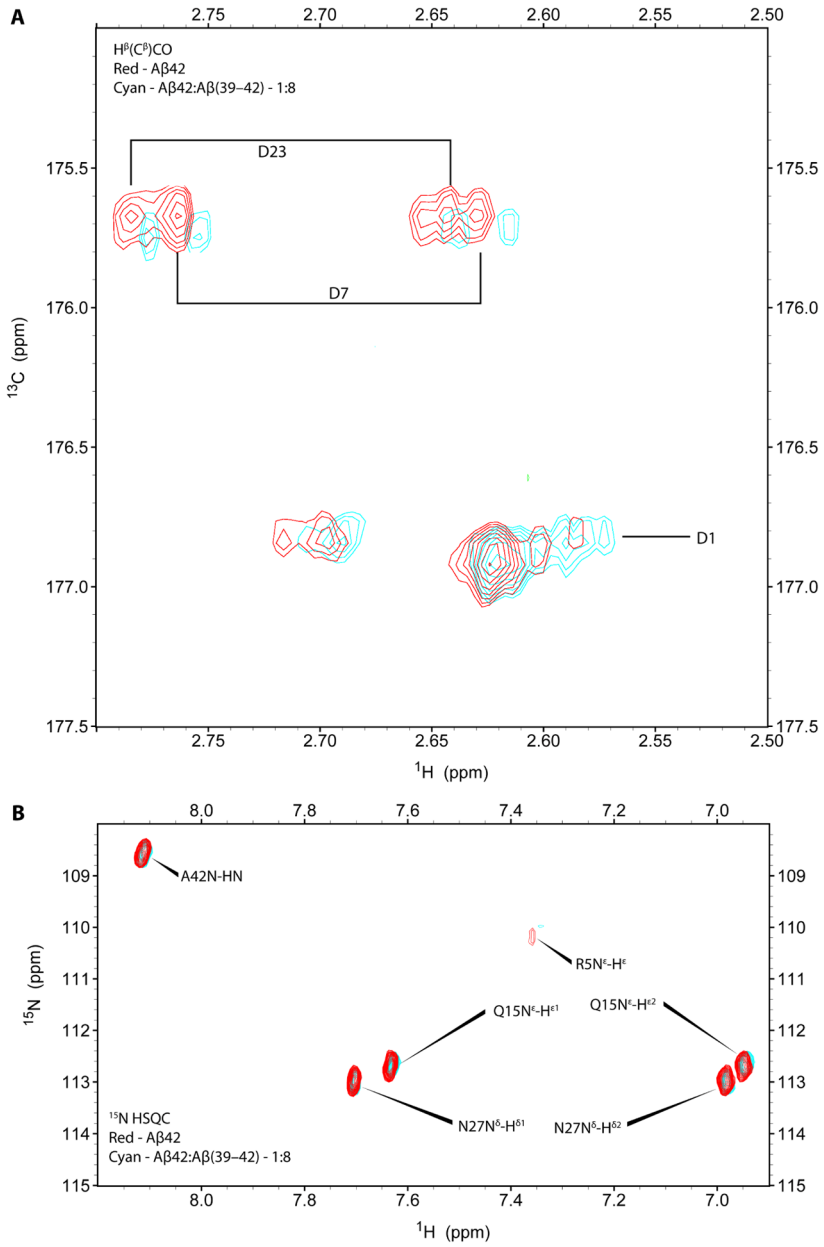

Figure 4. Aβ(39–42) binding site on Aβ42 determined by solution-state 2D NMR

Aβ42 resonances were measured in the absence (red) or presence (cyan) of 8-fold excess Aβ(39–42). A) 2D ^{13}C-^{1}H HSQC spectrum of Aβ42 in the absence or presence of Aβ(39–42) at 4°C. $H^{\beta}(C^{\beta})CO$ experiments detected upfield movement and reduced intensity of chemical shifts for the side-chains of D1, D7, and D23 upon addition of Aβ(39–42). B) 2D ^{15}N-^{1}H HSQC spectra of Aβ42 in the absence or presence of Aβ(39–42) detected upfield movement and reduced intensity of chemical shifts for the N^{ε}-H^{ε} crosspeak of R5.

Table 1

Physicochemical characteristics of Aβ(39–42).

Criterion	Recommended Value	Aβ(39–42)
Lipinski's rule of 5[26]		
MW	< 500	400.5
ClogP	< 5	−0.3
H-bond donors	≤ 5	5
H-bond acceptors	≤ 10	9
tPSA (Å^2)	≤ 140[27]	150.62

Table 2

Sequences, masses, and IC_{50} values of Aβ(39–42) and derivatives.

Sequence	Calculated mass	Observed mass[b]	IC_{50} (μM) (MTT)	IC_{50} (μM) (LDH)
VVIA	401.5	401.2	21 ± 6	16 ± 3
AVIA	373.5	373.0	53 ± 10	22 ± 5
V**A**IA	373.5	373.2	15 ± 3	14 ± 2
VV**A**A	359.4	359.1	n.d.	n.d.
VVIA[a]	401.5	401.2	n.d.	n.d.
AC-VVIA	443.6	443.4	n.d.	n.d.
VVIA-$\mathbf{NH_2}$	399.5	400.1	28 ± 7	30 ± 5
AIVV	401.5	401.3	14 ± 1	22 ± 3
AC-AIVV	443.5	443.1	n.d.	n.d.
AIVV-$\mathbf{NH_2}$	399.5	400.2	20 ± 4	16 ± 3

[a] Lower-case letters represent *D*-configuration.

n.d. – not determined.